

Mg-rich wolfeite, $(\text{Fe}^{\text{II}}, \text{Mg})_2(\text{PO}_4)(\text{OH})$: structure refinement and Raman spectroscopic data

Uwe Kolitsch

Universität Wien, Institut für Mineralogie und
Kristallographie, Geozentrum, Althanstrasse 14,
A-1090 Wien, Austria

Correspondence e-mail:
uwe.kolitsch@univie.ac.at

Key indicators

Single-crystal X-ray study

$T = 293 \text{ K}$

Mean $\sigma(\text{P}-\text{O}) = 0.001 \text{ \AA}$

Disorder in main residue

R factor = 0.022

w R factor = 0.065

Data-to-parameter ratio = 17.3

For details of how these key indicators were
automatically derived from the article, see
<http://journals.iucr.org/e>.

Mg-rich wolfeite [diiron(II) hydroxide phosphate], $(\text{Fe}^{\text{II}}, \text{Mg})_2(\text{PO}_4)(\text{OH})$, from the Big Fish River area, Yukon Territory, Canada, is isotypic with its Mn^{II} -dominant analogue triploidite. The framework structure contains edge- and corner-sharing, distorted $\text{MO}_4(\text{OH})$ and $\text{MO}_4(\text{OH})_2$ ($M = \text{Fe}^{\text{II}}$ or $\text{Fe}^{\text{II}}, \text{Mg}$) polyhedra linked by fairly regular PO_4 tetrahedra. All atoms are on general positions. Four of the eight independent Fe sites contain between 9 and 25% Mg substituting for Fe. Two of these four sites show distorted trigonal-bipyramidal coordination, whereas the remaining two sites show distorted octahedral coordination. The average $(\text{Fe}^{\text{II}}, \text{Mg})-\text{O}$ bond length decreases with increasing Mg content. Average P—O distances range between 1.538 and 1.543 Å. The hydrogen bonds are all strongly bent and weak, with $\text{O} \cdots \text{O}$ distances $> 2.73 \text{ \AA}$, an observation confirmed by single-crystal Raman spectroscopic data which show five bands due to O—H stretching vibrations between 3478 and 3557 cm^{-1} .

Received 28 July 2003

Accepted 7 August 2003

Online 15 August 2003

Comment

Wolfeite, $(\text{Fe}^{\text{II}}, \text{Mn}^{\text{II}})_2(\text{PO}_4)(\text{OH})$ (Mandarino, 1999), is a rare iron phosphate mineral which occurs as a metasomatic alteration phase in pegmatites, and also rarely in hydrothermal veins, phosphatic nodules in shales, and amphibolite-facies metamorphosed iron formations (Anthony *et al.*, 2000; Masau *et al.*, 2000; Stalder & Rozendaal, 2002, and references therein). Wolfeite is a member of a large family of compounds with the general formula $M_2^{\text{II}}(\text{XO}_4)\text{Z}$, where $M = \text{Fe}, \text{Mn}, \text{Mg}, \dots$; $X = \text{P}, \text{As}, \dots$; and $Z = \text{F}, \text{OH}, \text{O}, \text{Cl}$ *etc.* According to the crystal-chemical classification of Strunz & Nickel (2001), wolfeite belongs to the triploidite group of minerals, whose other members are triploidite [$(\text{Mn}^{\text{II}}, \text{Fe}^{\text{II}})_2(\text{PO}_4)(\text{OH})$; Waldrop, 1970], wagnerite [$\text{Mg}_2(\text{PO}_4)\text{F}$; Coda *et al.*, 1967], staněkite [$(\text{Mn}, \text{Fe}^{\text{II}}, \text{Mg})\text{Fe}^{\text{III}}(\text{PO}_4)\text{O}$; Keller *et al.*, 1997] and sarkinite [$\text{Mn}^{\text{II}}_2(\text{AsO}_4)(\text{OH})$; Dal Negro *et al.*, 1974]. Various synthetic compounds are also isotypic with triploidite [*e.g.* $\beta\text{-Mg}_2(\text{PO}_4)(\text{OH})$ (Raade & Rømming, 1986) and $\text{Zn}_2(\text{PO}_4)(\text{F}, \text{OH})$ (Taasti *et al.*, 2002)]. All triploidite-type compounds crystallize with space group $P2_1/a$ and have similar unit-cell parameters. The common structure type is closely related to that of triplite, $(\text{Mn}^{\text{II}}, \text{Fe}^{\text{II}})_2(\text{PO}_4)\text{F}$ (space group $I2/a$; Waldrop, 1969; alternative setting in $C2/c$ for synthetic triplite by Rea & Kostiner, 1972).

The crystal structure of wolfeite has not been studied thus far, although X-ray powder diffraction data and unit-cell parameters have been provided by Frondel (1949), Antenucci *et al.* (1989), and Masau *et al.* (2000). The present article reports the results of a single-crystal structure refinement and of single-crystal Raman spectroscopic studies of a Mg-rich

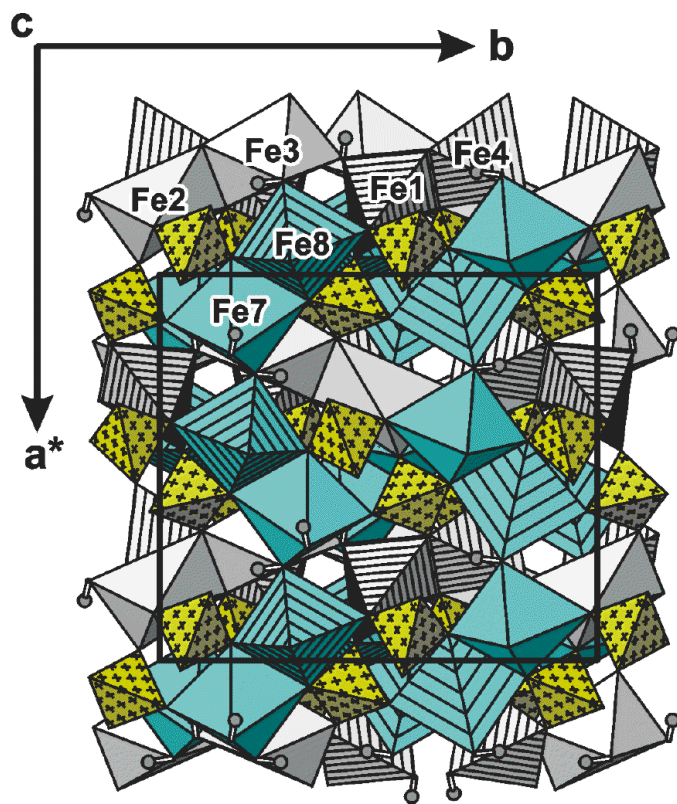


Figure 1

View along [001] of the complex framework structure of Mg-rich wolfeite from the Big Fish River area, Yukon Territory, Canada. Edge- and corner-sharing, distorted $MO_4(OH)$ ($M = Fe^{II}, Mg$) trigonal bipyramids (striped) and $MO_4(OH)_2$ octahedra (unmarked) are corner-linked to PO_4 tetrahedra (yellow, marked with crosses). All Mg-containing polyhedra are shown in blue. The unit cell is outlined.

wolfeite sample from the Big Fish River area, Yukon Territory, Canada (Robertson, 1982; Robinson *et al.*, 1992). The article supplements an earlier study of the crystal structure and IR spectra of a Mg-rich satterlyite, $(Fe, Mg)_{12}(PO_3OH)(PO_4)_5(OH, O)_6$, from the same locality (Kolitsch *et al.*, 2002).

At the Big Fish River area, the mineral is a common constituent of epigenetic phosphatic nodules and forms divergent, columnar aggregates of crude, glassy, light brown to clove-brown crystals up to several centimetres in length. Crystallization occurred at temperatures of about 453 to 473 K, according to fluid inclusion studies (Robinson *et al.*, 1992). Previous electron microprobe analyses of wolfeite from this locality yielded an average formula close to $(Fe_{1.65}Mg_{0.20}Mn_{0.15})_2(PO_4)(OH_{0.95}F_{0.05})$ (Robinson *et al.*, 1992). The presently studied sample is from the collection of the author, and its appearance closely fits the published descriptions (Robinson *et al.*, 1992). The chemical composition of the sample has been characterized by semiquantitative SEM-EDS data which revealed major Fe and P, minor Mg and only very small amounts of Mn (ratio Fe:Mn *ca.* 13:1), and insignificant compositional inhomogeneities. The EDS-based chemical composition is in good agreement with the formula subsequently derived from the structure refinement.

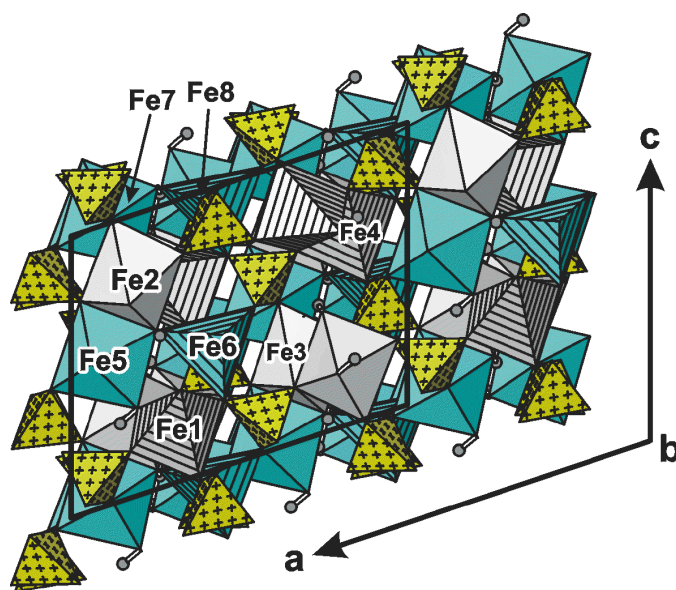


Figure 2

The complex crystal structure of Mg-rich wolfeite, projected along [010]. For key see Fig. 1.

Mg-rich wolfeite is confirmed to be isotypic with triploidite $(Mn^{II}, Fe^{II})_2(PO_4)(OH)$; space group $P2_1/a$; Waldrop, 1970). It has a complex framework structure based on edge- and corner-sharing, distorted $MO_4(OH)$ and $MO_4(OH)_2$ polyhedra ($M = Fe^{II}, Mg$), corner-linked to PO_4 tetrahedra (Figs. 1, 2). For detailed descriptions of the connectivity, the reader is referred to the previous reports on the isotypic members of the triploidite group (see above). The present paper restricts itself to the Mg distribution and the hydrogen bonding in Mg-rich wolfeite. To facilitate comparisons, the atomic coordinates and the labeling used by Waldrop (1970) for triploidite were adopted for Mg-rich wolfeite, except for the H atoms which had not been located during the earlier study of triploidite. The crystal structure of Mg-rich wolfeite contains eight non-equivalent Fe sites, four P sites, twenty O sites, and four H sites (belonging to OH groups). All atoms are on general positions. The Fe sites Fe1, Fe4, Fe6, and Fe8 are all five-coordinated (with distorted trigonal-bipyramidal geometry), whereas the remaining Fe sites show distorted octahedral coordination (with OH groups in the *cis* configuration). Site occupancy refinements demonstrated that the considerable Mg present in the structure strictly prefers the following four out of the eight Fe sites: Fe5, Fe6, Fe7, and Fe8. The refined Fe:Mg ratios at these sites range between approximately 0.76:0.24 (Fe6) and 0.90:0.10 (Fe5) (Table 1). Thus, the Mg substitutes for Fe on two five-coordinated and two six-coordinated sites, and therefore exhibits no preference for a certain coordination environment. A view of the polyhedral arrangement along [001] (Fig. 1) shows that the Mg-bearing polyhedra $Fe_7O_4(OH)_2$ and $Fe_8O_4(OH)$ (shown in blue) are connected into undulating chains running parallel to [100], by alternately sharing corners and edges. The other two Mg-bearing polyhedra, $Fe_5O_4(OH)_2$ and $Fe_6O_4(OH)$, are connected *via* a shared corner on a level below the undulating chain (Fig. 2);

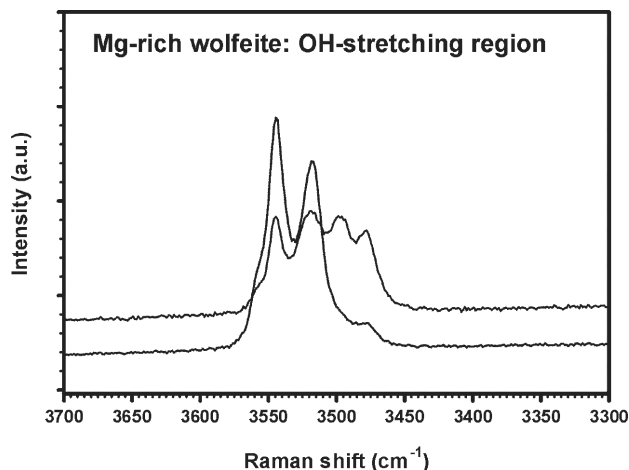


Figure 3

Two single-crystal laser-Raman spectra of Mg-rich wolfeite from the Big Fish River area, Yukon Territory, Canada, in the OH stretching region. See text for details and band positions.

the Fe5–Fe6 vector also runs approximately parallel to [100]. The two polyhedra most rich in Mg, $\text{Fe}_6\text{O}_4(\text{OH})$ and $\text{Fe}_7\text{O}_4(\text{OH})_2$, are not connected to each other. Seemingly, the structure thereby avoids misfit-induced strain in the structure.

Average Fe–O distances for the five-coordinated sites are 2.103 (Fe1), 2.109 (Fe4), 2.062 (Fe6), and 2.077 Å (Fe8). The six-coordinated sites show average Fe–O distances of 2.188 (Fe2), 2.180 (Fe3), 2.152 (Fe5), and 2.139 Å (Fe7). All Mg-containing sites have shorter average distances than their Mg-free counterparts. This is consistent with the fact that the commonly observed average $^{60}\text{Fe}^{\text{II}}\text{–O}$ distance, 2.138 Å, is distinctly larger than the corresponding value for Mg, 2.085 Å (Baur, 1981). Because Fe^{II} is generally considered an actively distorting cation which prefers distorted octahedra if present, it also comes as no surprise that the six-coordinated Fe sites containing no Mg (Fe2 and Fe3) exhibit a higher bond-length distortion than both their Mg-containing counterparts (Fe5 and Fe7). Hydrothermal syntheses would be necessary to determine how much Mg can substitute for Fe^{II} in synthetic wolfeite under specified p – T conditions. The unit-cell volume of the presently studied Mg-rich wolfeite, 1493.9 (5) Å³, is distinctly smaller than previously reported cell volumes for wolfeites very poor in Mg [1521.74 Å³ (Antenucci *et al.*, 1989) and 1523.0 (5) Å³ (Masau *et al.*, 2000)]. The cell edge most strongly affected by the Mg incorporation is the a edge whose length decreases by nearly 3% by comparison to the literature data (Antenucci *et al.*, 1989; Masau *et al.*, 2000). This is convincingly explained by the arrangement along [100] of the Mg-containing polyhedra (*cf.* Figs. 1 and 2).

The four non-equivalent PO_4 tetrahedra all show fairly regular geometries (Table 1). Average P–O distances are 1.543 (P1), 1.538 (P2), 1.540 (P3), and 1.542 Å (P4). The hydrogen bonding scheme in Mg-rich wolfeite is somewhat unusual. The hydrogen bonds are all weak, with O···O distances between 2.73 and *ca.* 3.1 Å. Each OH group is bonded to three cations (Fe or Mg), *i.e.* its bond-valence requirements are basically satisfied, and formally one might

not expect the H atoms to form any hydrogen bond at all. However, the framework topology allows a larger number of weak hydrogen bonds, and, in fact, three of the four OH groups are involved in bifurcated, possibly even trifurcated hydrogen bonds which are strongly bent (Table 2). Only the bond donated by the O20–H4 group has a single acceptor atom, O7. None of the four (freely refined) H sites shows any unusual displacement parameters, and O–H distances are within a very narrow range between 0.78 and 0.80 Å (Table 2). In isotypic synthetic $\beta\text{-Mg}_2(\text{PO}_4)(\text{OH})$ (Raade & Rømming, 1986), the hydrogen bonds are also weak and strongly bent (O–H–O angles range between 116 and 144°, similar to the situation in Mg-rich wolfeite). The hydrogen bonding scheme in triploidite is unknown because positions of H atoms could not be located during the structure determination by Waldrop (1970).

A further, spectroscopic characterization of the hydrogen bonds was obtained by laser Raman spectroscopy. Spectra of a single-crystal fragment were recorded in the range from 4000 to 100 cm^{-1} with a Renishaw M1000 MicroRaman Imaging System using a laser wavelength of 633 nm and excitation through a Leica DMLM optical microscope (spectral resolution $\pm 2 \text{ cm}^{-1}$, minimum lateral resolution *ca.* 2 μm , unpolarized laser light, 180° backscatter mode, random sample orientation). Two representative spectra, given in Fig. 3, were recorded from different, but unspecified cleavage planes. The spectra show four sharp bands (and one shoulder) due to O–H stretching vibrations at 3557 (shoulder), 3544, 3518, 3497 (only seen in one spectrum due to orientation effects), and 3478 cm^{-1} . Using the correlation of O–H stretching frequencies and O···O hydrogen bond lengths in minerals by Libowitzky (1999), the observed O–H stretching frequencies in Mg-rich wolfeite would correspond to approximate O···O bond lengths ranging between 2.8 and 3.0 Å, in good agreement with the results of the structure refinement. In the powder infrared spectrum of isotypic synthetic $\beta\text{-Mg}_2(\text{PO}_4)(\text{OH})$, only two sharp bands at 3595 and 3580 cm^{-1} were observed (Raade & Rømming, 1986), thus indicating weaker hydrogen bonding than in Mg-rich wolfeite.

Experimental

Crystal data

$\text{Fe}_{1.84}\text{Mg}_{0.16}(\text{PO}_4)(\text{OH})$
 $M_r = 218.63$
 Monoclinic, $P2_1/a$
 $a = 12.274$ (2) Å
 $b = 13.169$ (3) Å
 $c = 9.754$ (2) Å
 $\beta = 108.64$ (3)°
 $V = 1493.9$ (6) Å³
 $Z = 16$

$D_x = 3.888 \text{ Mg m}^{-3}$
 Mo $K\alpha$ radiation
 Cell parameters from 5647 reflections
 $\theta = 2.0$ – 32.6°
 $\mu = 7.52 \text{ mm}^{-1}$
 $T = 293$ (2) K
 Fragment, yellow
 $0.18 \times 0.18 \times 0.13 \text{ mm}$

Data collection

Nonius KappaCCD diffractometer
 ψ and ω scans
 Absorption correction: multi-scan
 (HKL SCALEPACK;
 Otwinowski & Minor, 1997)
 $T_{\text{min}} = 0.294$, $T_{\text{max}} = 0.376$
 10662 measured reflections

5432 independent reflections
 4267 reflections with $I > 2\sigma(I)$
 $R_{\text{int}} = 0.014$
 $\theta_{\text{max}} = 32.6^\circ$
 $h = -18 \rightarrow 18$
 $k = -19 \rightarrow 19$
 $l = -14 \rightarrow 14$

Refinement

Refinement on F^2	$w = 1/[\sigma^2(F_o^2) + (0.034P)^2 + 0.36P]$
$R[F^2 > 2\sigma(F^2)] = 0.022$	where $P = (F_o^2 + 2F_c^2)/3$
$wR(F^2) = 0.065$	$(\Delta/\sigma)_{\max} = 0.003$
$S = 1.03$	$\Delta\rho_{\max} = 0.55 \text{ e } \text{\AA}^{-3}$
5432 reflections	$\Delta\rho_{\min} = -0.67 \text{ e } \text{\AA}^{-3}$
314 parameters	Extinction correction: <i>SHELXL97</i>
All H-atom parameters refined	Extinction coefficient: 0.00357 (15)

Table 1
Selected geometric parameters (Å).

Fe1—O20	2.0326 (13)	Fe6—O6	2.0482 (12)
Fe1—O10	2.0546 (12)	Fe6—O13	2.0665 (13)
Fe1—O15 ⁱ	2.0858 (13)	Fe6—O1	2.1604 (13)
Fe1—O6	2.1591 (12)	Fe7—O4 ^{vii}	2.0782 (12)
Fe1—O11	2.1827 (11)	Fe7—O19	2.0869 (12)
Fe2—O16 ⁱ	2.1124 (13)	Fe7—O16	2.1314 (13)
Fe2—O17 ⁱⁱ	2.1185 (13)	Fe7—O7	2.1464 (13)
Fe2—O12	2.1372 (11)	Fe7—O18 ⁱ	2.1478 (14)
Fe2—O18 ⁱⁱ	2.2029 (13)	Fe7—O3	2.2437 (13)
Fe2—O9	2.2526 (12)	Fe8—O19 ^{viii}	2.0167 (13)
Fe2—O5 ⁱⁱ	2.3059 (12)	Fe8—O8	2.0580 (12)
Fe3—O14 ⁱⁱⁱ	2.1054 (13)	Fe8—O3 ^{vii}	2.0666 (11)
Fe3—O9	2.1058 (11)	Fe8—O15	2.0893 (13)
Fe3—O19	2.1237 (13)	Fe8—O4	2.1543 (12)
Fe3—O7	2.2139 (12)	P1—O7 ^{ix}	1.5327 (13)
Fe3—O20	2.2433 (13)	P1—O9	1.5397 (12)
Fe3—O12	2.2877 (12)	P1—O2	1.5501 (12)
Fe4—O18	2.0320 (13)	P1—O13	1.5508 (12)
Fe4—O11	2.0391 (12)	P2—O1	1.5343 (12)
Fe4—O13 ^{iv}	2.0660 (13)	P2—O14	1.5359 (12)
Fe4—O8	2.1862 (12)	P2—O8 ^x	1.5366 (13)
Fe4—O10	2.2195 (11)	P2—O10	1.5464 (11)
Fe5—O17	2.1131 (12)	P3—O5 ^{xi}	1.5295 (13)
Fe5—O5	2.1223 (13)	P3—O4	1.5379 (12)
Fe5—O20 ^{iv}	2.1269 (14)	P3—O16	1.5405 (12)
Fe5—O14	2.1733 (13)	P3—O11	1.5529 (11)
Fe5—O2 ^v	2.1781 (12)	P4—O12	1.5322 (11)
Fe5—O2 ^{vi}	2.2006 (13)	P4—O6 ^{xii}	1.5407 (13)
Fe6—O17 ⁱⁱⁱ	2.0090 (13)	P4—O15 ⁱⁱ	1.5476 (12)
Fe6—O1 ^v	2.0240 (12)	P4—O3	1.5496 (12)

Symmetry codes: (i) $\frac{1}{2} - x, \frac{1}{2} + y, -z$; (ii) $x, 1 + y, z$; (iii) $\frac{1}{2} - x, \frac{1}{2} + y, 1 - z$; (iv) $\frac{1}{2} - x, y - \frac{1}{2}, 1 - z$; (v) $-x, 1 - y, 1 - z$; (vi) $x, y - 1, z$; (vii) $1 - x, 1 - y, -z$; (viii) $\frac{1}{2} - x, y - \frac{1}{2}, -z$; (ix) $x - \frac{1}{2}, \frac{3}{2} - y, z$; (x) $x - \frac{1}{2}, \frac{1}{2} - y, z$; (xi) $\frac{1}{2} + x, \frac{1}{2} - y, z$; (xii) $\frac{1}{2} + x, \frac{3}{2} - y, z$.

Table 2
Hydrogen-bonding geometry (Å, °).

D—H...A	D—H	H...A	D...A	D—H...A
O17—H1...O9 ⁱ	0.79 (3)	2.23 (3)	2.7343 (17)	122 (2)
O17—H1...O1 ⁱⁱ	0.79 (3)	2.32 (3)	2.7798 (17)	118 (2)
O17—H1...O10 ⁱⁱⁱ	0.79 (3)	2.50 (3)	3.1627 (18)	142 (3)
O18—H2...O5	0.79 (3)	2.33 (3)	2.8418 (17)	124 (3)
O18—H2...O4 ⁱⁱⁱ	0.79 (3)	2.58 (3)	2.9803 (19)	113 (2)
O19—H3...O12	0.78 (3)	2.32 (3)	2.8057 (17)	122 (2)
O19—H3...O4 ^{iv}	0.78 (3)	2.39 (2)	2.7978 (17)	114 (2)
O19—H3...O11 ^{iv}	0.78 (3)	2.40 (3)	3.0609 (17)	143 (2)
O20—H4...O7	0.80 (2)	2.21 (2)	2.7313 (17)	123 (2)

Symmetry codes: (vi) $x, y - 1, z$; (iv) $\frac{1}{2} - x, y - \frac{1}{2}, 1 - z$; (x) $x - \frac{1}{2}, \frac{1}{2} - y, z$; (i) $\frac{1}{2} - x, \frac{1}{2} + y, -z$.

H atoms were freely refined. The Fe:Mg ratios of the four Mg-containing sites, Fe5, Fe6, Fe7 and Fe8, were freely refined, assuming full occupancy of each site. All atomic displacement ellipsoids were regular.

Data collection: *COLLECT* (Nonius, 2002); cell refinement: *HKL SCALEPACK* (Otwinowski & Minor, 1997); data reduction: *HKL DENZO* (Otwinowski & Minor, 1997) and *SCALEPACK*; program(s) used to solve structure: *SHELXS97* (Sheldrick, 1997); program(s) used to refine structure: *SHELXL97* (Sheldrick, 1997); molecular graphics: *ATOMS* (Shape Software, 1999).

Financial support by the German Science Foundation (DFG) and the Austrian Science Foundation (FWF) (grant P15220-N06) is gratefully acknowledged.

References

Antenucci, D., Fontan, F. & Fansolet, A. M. (1989). *Powder Diffract.* **4**, 34–35.

Anthony, J. W., Bideaux, R. A., Bladh, K. W. & Nichols, M. C. (2000). *Handbook of Mineralogy*. Vol. IV: *Arsenates, Phosphates, Vanadates*. Tucson: Mineral Data Publishing.

Baur, W. H. (1981). *Structure and Bonding in Crystals*, Vol. II, edited by M. O’Keeffe and A. Navrotsky, pp. 31–52. New York: Academic Press.

Coda, A., Giuseppetti, G. & Tadini, C. (1967). *Atti Accad. Naz. Lincei, Rend. Cl. Sci. Fis. Mater. Natur.* **43**, 212–224.

Dal Negro, A., Giuseppetti, G. & Martin Pozas, J. M. (1974). *Tschermaks Mineral. Petrogr. Mitt.* **21**, 246–260.

Frondel, C. (1949). *Am. Mineral.* **34**, 692–705.

Keller, P., Fontan, F., Velasco-Roldan, F. & Melgarejo i Draper, J. C. (1997). *Eur. J. Mineral.* **9**, 475–482.

Kolitsch, U., Andrut, M. & Giester, G. (2002). *Eur. J. Mineral.* **14**, 127–133.

Libowitzky, E. (1999). *Monatsh. Chem.* **130**, 1047–1059.

Mandarino, J. A. (1999). *Fleischer’s Glossary of Mineral Species 1999*. Tucson: The Mineralogical Record Inc.

Masau, M., Staněk, J., Černý, P. & Chapman, R. (2000). *J. Czech. Geol. Soc.* **45**, 159–173.

Nonius (2002). *COLLECT*. Nonius BV, Delft, The Netherlands.

Otwinowski, Z. & Minor, W. (1997). *Methods in Enzymology*, Vol. 276, *Macromolecular Crystallography*, Part A, edited by C. W. Carter and R. M. Sweet, pp. 307–326. New York: Academic Press.

Raade, G. & Rømming, C. (1986). *Z. Kristallogr.* **177**, 15–26.

Rea, J. R. & Kostiner, E. (1972). *Acta Cryst.* **B28**, 2525–2529.

Robertson, B. T. (1982). *Can. Mineral.* **20**, 177–187.

Robinson, G. W., Van Velthuizen, J., Ansell, H. G. & Sturman, B. D. (1992). *Mineral. Rec.* **23**, 4–47.

Sheldrick, G. M. (1997). *SHELXS97* and *SHELXL97*. University of Göttingen, Germany.

Shape Software (1999). *ATOMS for Windows and Macintosh*. Version 5.0.4. Shape Software, Kingsport, TN 37663, USA.

Stalder, M. & Rozendaal, A. (2002). *Mineral. Mag.* **66**, 915–927.

Strunz, H. & Nickel, E. H. (2001). *Strunz Mineralogical Tables*. Stuttgart: E. Schweizerbart’sche Verlagsbuchhandlung.

Taasti, K. I., Christensen, A. N., Norby, P., Hanson, J. C., Lebeck, B., Jakobsen, H. J. & Skibsted, J. (2002). *J. Solid State Chem.* **164**, 42–50.

Waldrop, L. (1969). *Z. Kristallogr.* **130**, 1–14.

Waldrop, L. (1970). *Z. Kristallogr.* **131**, 1–20.